MAGNETICALLY LEVITATED ROTARY ARTIFICIAL HEART WITH AXIAL SUSPENSION MOTOR

Tsuyoshi Kato
Dept. of Mechanical Eng., Ibaraki University, Hitachi, Ibaraki-Pref., 316-8511 Japan
tykato@mech.ibaraki.ac.jp
Toru Masuzawa
Dept. of Mechanical Eng., Ibaraki University, Hitachi, Ibaraki-Pref., 316-8511 Japan
masuzawa@mech.ibaraki.ac.jp
Yohji Okada
Dept. of Mechanical Eng., Ibaraki University, Hitachi, Ibaraki-Pref., 316-8511 Japan
okada@mech.ibaraki.ac.jp

ABSTRACT
Axially levitated motors were developed to apply magnetic suspension technology to artificial hearts. The feasibility of the axially levitated motor was confirmed with a prototype motor and a magnetically suspended centrifugal pump was constructed with an improved motor. The axially levitated motor consists of a top stator, a levitated rotor, and a bottom stator. The maximum rotating speed of the levitated motor with pumping the water was 1700 rpm. The maximum amplitude of the rotor displacement in the axial direction was only 0.07 mm during pumping the water. The maximum head pressure and flow rate of the pump were 120 mmHg and 7.8 l/min, respectively. The developed pump displayed sufficient magnetic suspension ability and the potential as a ventricular assist device.

INTRODUCTION
The life time of a rotary blood pump for an artificial heart is mainly determined by the durability of mechanical parts such as bearings and seals. Especially, the life time of the seal used in a rotary blood pump is very short, specifically is few days [1,2]. The purpose of this study is to develop a durable centrifugal blood pump which are eliminated mechanical parts by using self-bearing motor techniques. In this paper, a magnetically suspended centrifugal blood pump by using an axially levitated motor is reported.

MATERIALS AND METHODS
Principle
Figure 1 shows the principle of the axially levitated motor. The developed motor consists of a top stator, a levitated rotor, and a bottom stator. The levitated rotor is set between the top and the bottom stator. The rotor has four or eight thin neodymium permanent magnets on the surface faced on the bottom stator and has a yoke at the top stator side. The top stator has four permanent magnets to produce upward directional bias magnetic force to the rotor. The top stator also has two pairs of concentrated wound poles to control the tilt of the levitated rotor. The bottom stator produces the attractive force to control the axial position of the levitated rotor and also produces the rotating torque of the levitated rotor. The radial movement of the rotor is restricted by passive stability. The passive stability is improved by narrowing down the magnetic pass way at the yokes set on the top stator and the rotor. It is made to simplify the control system by reducing the number of control. Four eddy current sensors are used to measure the rotor position in the axial direction and its tilt angles.

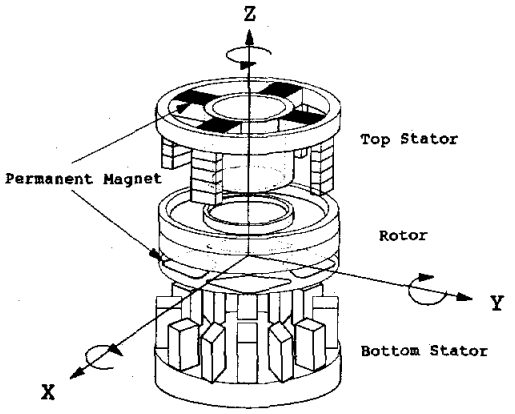

FIGURE 1: Principle of the axially levitated motor

Figure 2 shows the principle of the tilt control with the top stator. The bias magnetic flux is produced by the four permanent magnets in the top stator. A coil and an opposite coil are connected serially as a pair coil. The tilt of the rotor is regulated by increasing the magnetic flux in a pole and decreasing in another pole of a pair of coils. Two pairs of coils are used to regulate the tilt of the levitated rotor in x and y axes.
The bottom stator produces the attractive force to control the axial position of the levitated rotor and also produces the rotating torque of the levitated rotor. The axial position and the torque of the rotor are regulated independently by changing the magnitude and the phase difference of the magnetic flux with the vector control method [3]. The vector control method in the bottom stator is as follows.
The stator and the permanent magnet of the rotor are assumed to produce the following magnet flux density $B_s(\theta,t)$ and $B_r(\theta,t)$,

$$B_s(\theta,t) = B_S \cos(\omega t - M\theta) \quad (1)$$

$$B_r(\theta,t) = B_R \cos(\omega t - M\theta - \phi) \quad (2)$$

where B_S, B_R are peak density of magnetic flux produced by the stator electric magnet and the rotor permanent magnet, M is pole pair number of the rotor, ω is rotating speed of the rotor, θ is angular coordinate, and ϕ is the phase difference.
For simplicity, magnetic properties inside the rotor and the bottom stator are assumed to be homogenous and the reluctance is ignored when compared with that of the air gap. Then the axial force f_Z and the rotating torque τ_Z can be derived as follows,

$$f_Z = \frac{(r_2^2 - r_1^2)\pi}{4\mu_0}[B_R^2 + 2B_R B_S \cos M\phi + B_S^2] \quad (3)$$

$$\tau_Z = \frac{zM(r_2^2 - r_1^2)\pi}{2\mu_0} B_R B_S \sin M\phi \quad (4)$$

where r_1 and r_2 are the inner and outer radii of the rotor, z is the gap length which contains the thickness of the permanent magnets between the rotor and the bottom stator, μ_0 is the permeability of vacuum.
To control the axial position independently and the torque of the rotor separatory, $B_s(\theta,t)$ is divided into the direct axis component Bd and the quadrature axis component B_q corresponding to the flux direction of the permanent magnet. The direct axis component Bd and the quadrature axis component B_q are defined as follows,

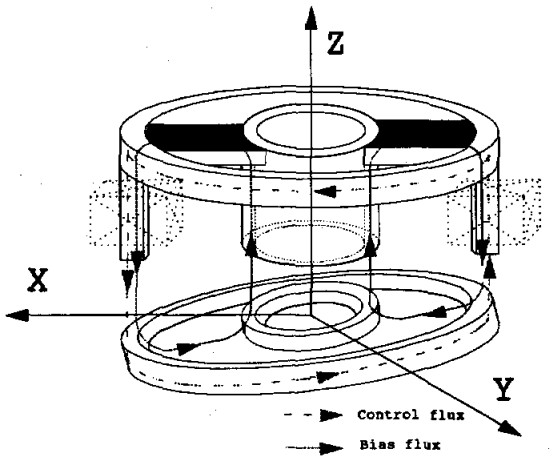

FIGURE 2: Principle of the tilt control with top stator

$$Bd = Bs \cos M\phi \quad (5)$$

$$Bq = Bs \sin M\phi \quad (6)$$

And u is defined as follows,

$$u = (B_R + B_d)^2 + B_q^2 \quad (7)$$

Then equation (3) and (4) can be derived as follows.

$$f_Z = \frac{(r_2^2 - r_1^2)\pi}{4\mu_0} u \quad (8)$$

$$\tau_Z = \frac{zM(r_2^2 - r_1^2)\pi}{2\mu_0} B_R B_q \quad (9)$$

Equation (8) shows that the axial attraction of the rotor can be controlled by changing only the magnitude of u. Equation (9) shows that the torque is also controlled by changing only the magnitude of the quadrature axis component B_q.
Necessary attraction f_Z and torque τ_Z are determined from the rotor position and the rotational condition, then u and B_q are calculated from equation (8) and (9). The magnitude of the direct axis component Bd is derived from substitution of calculated u and B_q in equation (7). The magnitude of the magnetic flux density B_S and the phase difference ϕ are derived from both components of the magnetic flux . The rotor levitation and rotation is controlled with a digital PID control algorithm using a digital signal processor.

Motor Design

When the centrifugal pump, which has an efficiency of 30 %, is driven with a head of 100 mmHg and a flow rate of 5 l/min, the motor must generate a power of 6 W [4]. The rotation speed in this condition is assumed to be 2000 rpm, at which the motor should generate a torque of 0.03 Nm. Therefore, the design specification for the levitated motor was set to produce a torque of 0.03 Nm with a rotating speed of 2000 rpm. The target attraction produced by the bottom stator was determined as 20 N when the air gap between the rotor and the stator is set to 2 mm. The number of turns in the coils and the geometric parameters of the permanent magnets were determined with equation (3) and (4).

Experimental Setup

Two motors were developed. First motor is a prototype motor to confirm feasibility of the method. Then, second motor was developed to improve the motor performance by redesigning the top and bottom stators. The attractive force produced by each stator was measured with a evaluation setup which has a miniature slider to guide the rotor. To evaluate the motor performance, the motor torque was measured with a evaluation setup which has a shaft to support the rotor.

Prototype Motor. Figure 3 shows top and bottom stators of the prototype motor. The diameter and the thickness of the top stator are 100 mm and 27 mm, respectively. Magnetic steel was used to make the core of the top stator. Ring shaped qermanent magnets made of Nd-F-B were set in the top stator. The number of turns in a coil for the tilt control was 224. The diameter and the thickness of the bottom stator are 55 mm and 30 mm. The bottom is made of magnetic steel and has six poles. The number of turns in the motor coil was 100. Four eddy current sensors were set outside of the top stator in the prototype motor.

The top stator could produce an attraction of 20 N with the 1.32 mm air gap between the rotor and the top stator. The bottom stator could produce an attraction form 18 N to 35 N with the 2 mm air gap. The prototype motor could generate a torque of 0.02 Nm with a rotating speed of 2000 rpm. The rotor could be driven up to a rotating speed of 800 rpm without touching anywhere in the air. The feasibility of the axially levitated motor could be confirmed with prototype motor. But both stator did not have sufficient performance.

Improved Motor. Figure 4 shows the improved motor. Magnetic field analysis was performed with commercial software *Ansys* because the attractive force produced by the top stator of the prototype motor was not sufficient. A optimized parameters are the cross-sectional area of

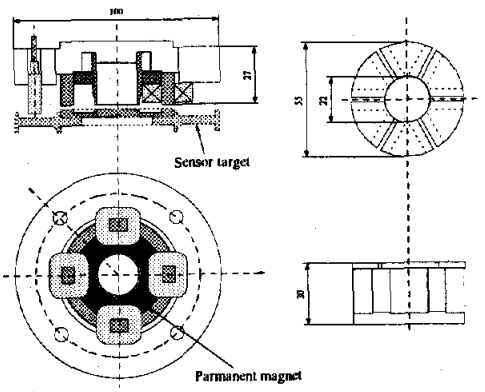

Top stator Bottom stator

FIGURE 3: Prototype motor

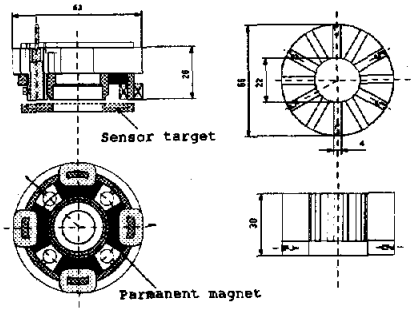

Top stator Bottom stator

FIGURE 4: Improved motor

the magnetic circuit and the size of permanent magnets. The improved motor was redesigned in consideration of the analysis result. The diameter and the thickness of the top stator of the improved motor are 63 mm and 26 mm, respectively. Magnetic steel was also used to make the core of the top stator of the improved motor. Four permanent magnets made of Nd-F-B were set in the top stator. Four eddy current sensors were set between the permanent magnets. The number of turns in a coil of the improved motor for the tilt control was 224. The bottom stator of the improved motor is made of laminated steels to decrease the eddy current loss. Thin laminated steel was wound like a tree ring and poles were constructed by wire electrical discharge machining. Two kinds of the bottom stator were developed. First stator has six poles to confirm the reduction in the eddy current loss. Second stator has twelve poles to change from four-pole motor into eight-pole motor to improve torque performance. The diameter and the thickness of both bottom stators are 55 mm and 30 mm. The number of turns in the motor coil was 100.

Rotor. Figure 5 shows the rotor construction. The diameter and thickness of the rotor are 59 mm and 19 mm, respectively. The rotor has the yoke part on the top stator side and the permanent magnet part on the bottom stator side. Four thin permanent magnets were used for four-pole motor. Eight permanent magnets were mounted for eight-pole motor. The rotor has a spacer of the thickness 5 mm between the yoke part and the magnet part.

Impeller. Figure 6 shows the impeller construction. A closed type impeller with six vanes was constructed between the yoke part and the permanent magnet part of the rotor. The size of the rotor-impeller is the same size as the rotor. A hole with a diameter of 15 mm was constructed as inlet eye at the center of the yoke. There is also a hole of the same size at the bottom side to wash out behind the impeller.

Magnetically levitated rotary Pump. Figure 7 shows the prototype pump with the axially levitated motor, which consists of the improved stators and the levitated rotor. A pump casing was constructed between the top and the bottom stators and the rotor-impeller was enclosed in the casing to build a magnetically suspended centrifugal blood pump. An inlet port of the pump penetrated the center of the cylindrical yoke of the top stator. An outlet port was set on circumferential sidewall of the casing. The diameter and the height of the pump are 81 mm and 65.5 mm, respectively. The axial gap between the rotor and the stators is 2 mm. The axial gap between the rotor and the pump casing is 0.4 mm. The radial gap between the rotor and the pump casing is 1.5 mm. A rotary encoder with a hall sensor was set at the circumference of the rotor to measure and control the rotating speed. The magnetic suspension ability and the pump performance of the pump were evaluated with a closed mock loop circuit filled with the water. The rotor displacement was measured with eddy current sensors to evaluate the magnetic suspension ability. The head pressure at the inlet and outlet was measured with pressure gauges and the flow rate of the pump was measured with a propeller flow meter. Input energy into the top and bottom stator was measured with a digital power meter.

RESULTS

Self-bearing Motor Performance

Figure 9 shows the relationship between attractive force produced by each top stator and the air gap length. The top stator of the prototype motor could produce an attraction of 13 N with the 2 mm air gap between the rotor and the top stator. The top stator of the improved motor could produce an attraction of 19 N with the 2

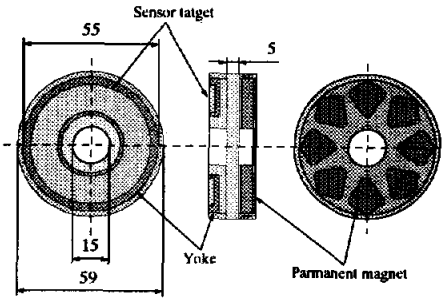

Top stator side Bottom stator side

FIGURE 5: Rotor construction

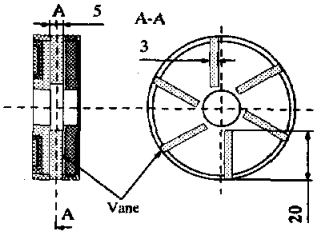

FIGURE 6: Impeller construction

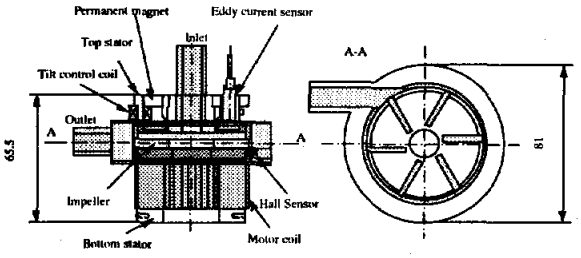

FIGURE 7: Prototype pump with the axially levitated motor

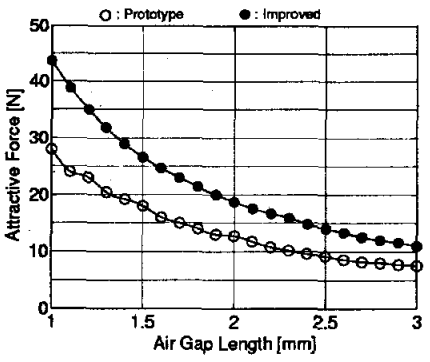

FIGURE 9: Measured attractive force produced by the top stators

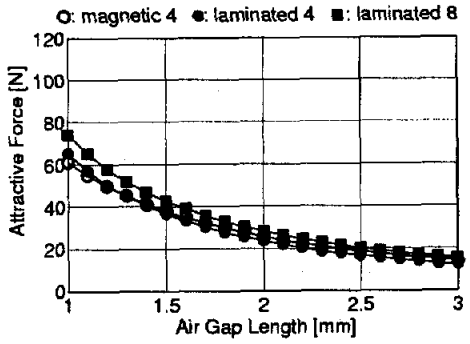

FIGURE 10: The attractive force produced by the bottom stators with 1 A coil current

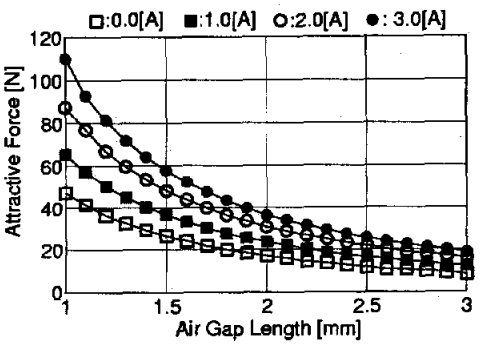

FIGURE 11: The attractive force produced by the bottom stator

mm air gap between the rotor and the top stator.

Figure 10 shows the relationship between attractive force produced by each bottom stator and the air gap length with a coil current of 1 A. Every bottom stator could produce a design target torque of 20 N.

Figure 11 shows the change in attractive force as the air gap length and exciting current of the improved bottom stator were changed. The bottom stator of the improved motor could produce an attraction form 18 to 35 N with the 2 mm air gap.

Figure 12 shows the motor torque performance. The four-phase motor made of magnetic steel could generate a torque of 0.02 Nm, the four-phase motor made of laminated steels could generate a torque of 0.04 Nm, the eight-phase motor made of laminated steels could generate a torque of 0.04 Nm with a rotating speed of 2000 rpm.

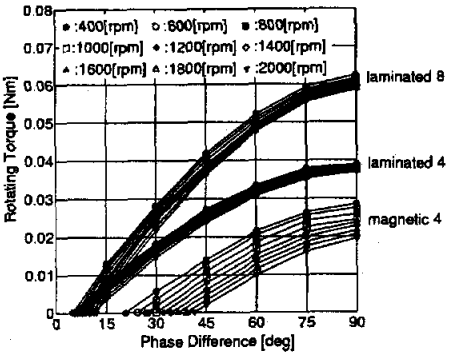

FIGURE 12: Generated torque of the developed motor

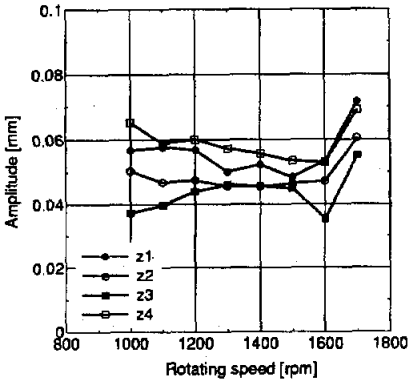

FIGURE 13: Maximum oscillation amplitude of the levitated rotor in axial direction

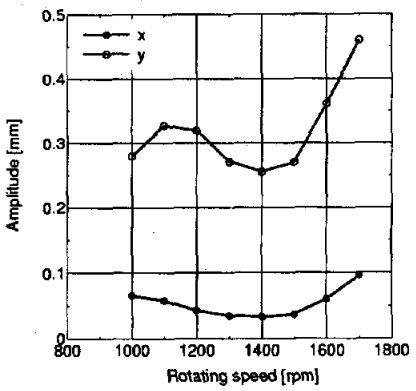

FIGURE 14: Maximum oscillation amplitude of the levitated rotor in radial direction

Suspension and Pump Performance

Figure 13 and 14 show the change in axial and radial maximum oscillation amplitude of the levitated rotor produced by increasing the rotating speed during pumping the water. The rotor could be driven up to a rotating speed of 1600 rpm without touching anywhere. The rotor touched the pump casing when the rotating speed exceeded 1700 rpm. The maximum amplitude of the levitated rotor displacement in the axial direction

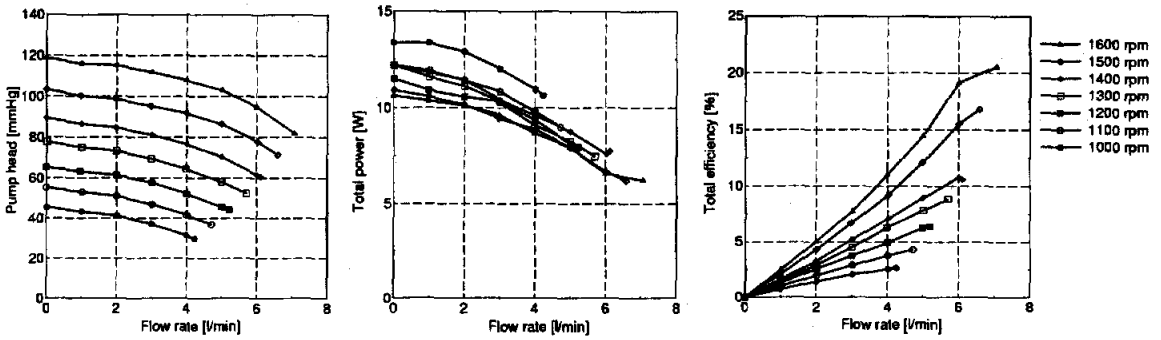

FIGURE 15: HQ characteristics, Total power consumption and Total efficiency

was 0.07 mm, that in the radial direction was 0.46 mm during pumping the water. Figure 15 shows Head pressure-Flow rate (HQ) characteristics. The maximum head pressure and the maximum flow rate were 120 mm Hg and 7.2 L/min, respectively. Figure 16 and 17 show the total power consumption and the total efficiency of pump. The power consumption and the total efficiency including the magnetic levitation system were 8.5 W and 15 %, respectively, with a head pressure of 100 mmHg and a flow rate of 5 L/min as a typical usage condition of ventricular assist devices.

DISCUSSION

The top stator of the prototype motor could only produce half attractive force as much as the design point. Also the prototype motor could not produce sufficient torque corresponding with the design point. But the feasibility of the axially levitated motor could be confirmed with the prototype motor.

The top stator of the improved motor could produce attractive force as much as the design point. The reduction of torque in high speed could be almost eliminated by changing the bottom stator material from magnetic steel to laminated steels. Also the improved motor could produce a torque of more than 0.03 Nm at the design point. This result indicates that the bottom stator could be downsized in next developed.

The maximum oscillation amplitude of the rotor displacement during pumping in the axial and radial direction were small enough. The power consumption and the total efficiency were excellent enough, 8.5 W and 15 %, as a typical usage condition of ventricular assist devices. The developed pump has sufficient pump performance as a ventricular assist device. The rotor contacted with the pump casing as the rotating speed exceeded 1700 rpm. The reason arise from the mechanism of the levitation and torque control with the vector control method. This method firstly determine B_q depending on the necessary torque by using digital PID. The current of B_q through the bottom stator produce not only torque but also attractive force. If this attractive force exceed the bias force, the rotor will contact the bottom stator. This phenomena could be overcome by adjusting the magnitude of bias force to charge the air gap between the rotor and the top stator.

CONCLUSION

The axially levitated centrifugal blood pump was developed with magnetic suspension techniques. The levitated motor displayed sufficient motor torque as an actuator of a centrifugal blood pump. The developed pump displayed good magnetic suspension ability, low power consumption characteristics, and sufficient pump performance as a ventricular assist device. The axially levitated centrifugal blood pump has the potential as an artificial heart.

REFERENCES

1. Masuzawa, T., Kita, T., Magnetically Suspended Rotary Blood Pump with Radial Type Combined Motor-Bearing, Artificial Organs, 24(6), 468-474.
2. Masuzawa, T., Kita, T., An Ultradurable and compact Rotary Blood Pump with a Mgnetically Suspended Impeller in the Radial Direction, Artificial Organs, 25(5), 395-399
3. Ueno, T., Okada, Y., Characteristics of Axial Force and Rotating Torque and their Contorol of PM type Axial Gap Self-bearing Motor, T. IEE Japan, Vol. 119-D, No. 3, March, 1999.
4. Masuzawa, T., Taenaka, Y., Development of Totally Implantable Artificial Heart, Jpn J Artif Organs, 24(2), 377-382, 1995.